

Received May 27, 2021, accepted June 14, 2021, date of publication June 21, 2021, date of current version July 1, 2021.

Digital Object Identifier 10.1109/ACCESS.2021.3090780

An Online Flexible Sorting Model for Coal and Gangue Based on Multi-Information Fusion

ZIXIANG WANG^{ID}, SHUXIN XIE^{ID}, GUODONG CHEN^{ID}, WENZHENG CHI^{ID}, (Member, IEEE),
ZIHAO DING^{ID}, AND PENG WANG

Jiangsu Provincial Key Laboratory of Advanced Robotics, School of Mechanical and Electrical Engineering, Soochow University, Suzhou 215123, China

Corresponding authors: Guodong Chen (guodongxyz@163.com) and Wenzheng Chi (wzchi@suda.edu.cn)

This work was supported by the National Key Research and Development Program of China under Grant 2019YFB1310201.

ABSTRACT Coal is one of the most important sources in China. The separation of coal and gangue is a key link in coal mining, and its intellectualization promotes the intelligent development of coal mining. But it is difficult to sort coal and gangue quickly and accurately because of some reasons, such as fast running speed of belt, different shapes and sizes of gangue, and so on. To solve the problem, an online flexible sorting model based on multi-information fusion is proposed. We use a near-infrared camera to identify coal and gangue, and combine it with a depth camera to obtain the height and pose information of gangue. Besides, we analyze the factors that affect the trajectory of gangue before and after pneumatic separation, deduce the theoretical formula of horizontal movement distance of gangue pneumatic separation, establish the mathematical model of gangue flexible sorting, and carry out experiments of pneumatic separation with different shapes and sizes of gangue. Experimental data is used to realize error compensation of the model. Finally, experimental results verify that the gangue flexible sorting model improve the accuracy of gangue sorting effectively and sort gangue with different shapes and sizes accurately despite the high-speed movement of belt.

INDEX TERMS Gangue sorting, pneumatic separation, multi-information fusion, flexible sorting model.

I. INTRODUCTION

Gangue is solid substance that is produced during the process of coal production. When it is burned with coal, gangue will not only produce harmful substances but also seriously affect the combustion efficiency of coal. Therefore, the separation of coal and gangue is an indispensable link in the process of coal production [1], [2]. Traditional separation methods of coal and gangue are mainly manual selection, mechanical washing, ray recognition and mechanical vibration. The manual sorting method is gradually eliminated because of its poor working environment and low efficiency. Mechanical washing mainly includes the heavy medium method [3], jigging method [4] and flotation method [5], which have problems such as easy loss of separation equipment, waste of water resources, increase in production cost caused by drying treatment and medium recovery [6], [7]. The ray recognition [8] method is harmful to the human body, and the mechanical vibration [9] method is only applicable to a few scenes. In recent years, coal and gangue separation technology based on visual recognition has attracted many scholars because

of its advantages of no water, simple processing and low investment [10]–[12].

Aldrich *et al.* [13] employed machine vision and kernel methods for online analysis of coal on conveyor belts. Lei *et al.* [14] proposed a method for coal and gangue identification based on CNN. Dou *et al.* [15] extracted multiple features for coal and gangue classification under different working conditions and applied the relief-SVM method to find the optimal features and construct the best classifier to identify coal and gangue. Wang *et al.* [16] designed an intelligent coal and gangue sorting system based on EAIDK, which uses a camera to identify coal and gangue and a mechanical arm to track and sort gangue. Cao *et al.* [17] designed a multi-manipulator coal and gangue sorting system based on vision, which can efficiently and accurately sort gangue. Shang *et al.* [18] designed a Delta parallel robot for coal and gangue sorting to address the problems of low sorting speed and low intelligence of gangue sorting robots. Compared with the serial robot, its sorting speed and efficiency are greatly improved.

At present, the intelligent sorting system of coal and gangue based on vision mainly adopts the method of vision + mechanical arm to identify and sort coal and gangue. With the

The associate editor coordinating the review of this manuscript and approving it for publication was Jon Atli Benediktsson^{ID}.

gradual increase in the amount and intensity of coal mining, the requirements for coal and gangue separation efficiency are also gradually increasing, so the requirements of the belt speed and sorting efficiency of coal and gangue separation lines are also becoming increasingly higher. However, due to the different shapes and sizes of gangue, high speeds of belts and the large amount of gangue, it is difficult to realize the rapid and accurate sorting of gangue on a high-speed belt by using a mechanical arm. In this paper, the method of pneumatic separation is adopted to realize the separation of coal and gangue on the high-speed belt, and PLC is used to control the on-off mode of the solenoid valve to realize the control of high-pressure gas. Solenoid valves have the advantages of high response speed and stable and reliable action [19], which are suitable for rapid sorting of gangue on high-speed belts. Currently, the pneumatic separation method has been widely employed in the separation of seeds in agriculture and the recovery of useful substances in industrial wastes, but its application in the separation of coal and gangue is limited. Zhang *et al.* [20] realized the automatic separation of different seeds by means of pneumatic separation. Mehrdad Baigvand *et al.* [21] developed a fig grading system based on machine vision, which uses images of fruits to classify and uses pneumatic separation method to separate different types of figs. Bi *et al.* [22] proposed a method to recover copper and aluminum fragments from the crushed products of waste lithium iron phosphate batteries based on the aerodynamic principle, and established an aerodynamic separation model to determine the optimal wind speed.

Hayashi and Oki [23] clarified the influence of orifice plates on gas velocity distribution and particle characteristics through numerical simulation of airflow and gas-solid multiphase flow in vertical single column pneumatic separator. de Almeida *et al.* [24] simulated the aerodynamic classification of bagasse particles, and the established model has a good predictive ability for various fluidization processes of bagasse. Zheng *et al.* [25] deduced the theoretical formula of the pneumatic separation distance of gangue, which has important guiding significance for the pneumatic separation of gangue. On this basis, Zheng *et al.* [26] proposed two different pneumatic separation schemes, and compared them to clarify several important factors affecting the pneumatic separation distance of gangue.

However, the abovementioned research on the pneumatic separation method of gangue is mainly based on an ideal situation. The regular sphere is used to replace the gangue in the simulation experiment of pneumatic separation, and the same sorting scheme is adopted for all gangues. Actually, the size and posture of gangues are randomly distributed, so it is difficult to accurately sort different gangues with only one scheme. If the blowing volume is small, the large gangues may fall into the coal pile due to insufficient blowing force, which may cause mis-sorting. In contrast, a large blowing volume will cause not only the surrounding coal to be blown away but also a waste of energy. If gangues with different

shapes and sizes can be sorted to an appropriate position, different blowing strengths and schemes should be adopted.

Therefore, this paper proposes an online flexible sorting model for coal and gangue based on the fusion of near-infrared and depth image information. The gangue information obtained by the near infrared camera and depth camera are input into the flexible sorting model to obtain different sorting strategies for gangue of different shapes and sizes under different influencing factors and to ensure that different gangues can be sorted to an appropriate position. By analyzing the movement trajectories of gangues with different sizes and postures under different influencing factors, this paper establishes a mathematical model of the horizontal moving distance of gangue pneumatic separation and determines the optimal flexible sorting strategy for the pneumatic separation of gangues with different sizes to the appropriate position. As a result, the sorting accuracy is improved.

II. COMPOSITION AND PRINCIPLE OF HIGH-SPEED FLEXIBLE SORTING SYSTEM FOR COAL AND GANGUE

The intelligent sorting system of coal and gangue is mainly divided into two parts: a vision module and a sorting module. The vision module includes a near-infrared camera and a depth camera. A near-infrared camera is used to identify coal and gangue, which is not affected by changes in external light and can capture the energy of the object surface. It is more suitable for coal and gangue identification in the harsh scene of coal mines than visible light camera. The depth camera is employed to obtain the point cloud information of gangue. After processing and calculation, the center coordinates and height information of gangue are obtained. Then, by matching the information obtained by the two cameras, the classification of coal and gangue and the length, width and height of the target object can be obtained. According to the ratio and product of its length, width and height, the posture and mass of the gangue can be obtained. Considering that the gangue density may be different in different areas, different gangue density values can be substituted into calculation for different areas. This paper takes 1800 kg/m^3 as the reference value of gangue density and puts it into calculation. For middling coal (mixture of clean coal and gangue), this paper identifies it as coal. The sorting module adopts a self-designed array pneumatic separation device, as shown in Fig. 1. The device can be adjusted to an appropriate angle according to different belt speeds to carry out strategic blowing sorting for different gangues.

In this paper, the movement distance of gangue from the camera view to the pneumatic separation device is converted into pulse value. When the pulse value of belt movement recorded by encoder reaches the value, the solenoid valve is controlled to carry out pneumatic sorting, thus realizing the pneumatic separation of the target object in the process of movement.

This system focuses on the sorting of coal and gangue with diameters in the range of 50-200 mm. First, the raw coal is screened through the roller screen, and the coal and gangue

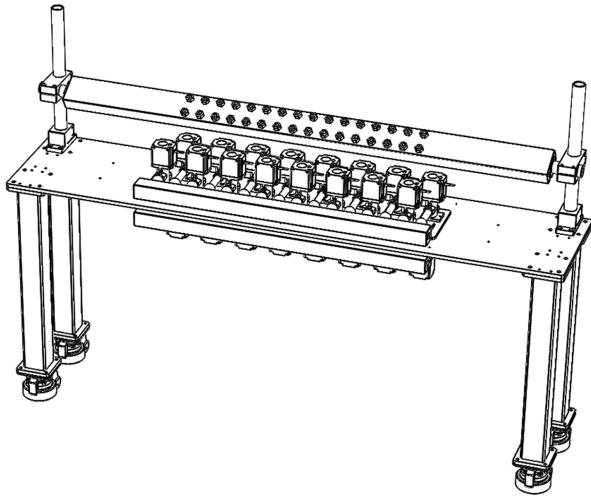


FIGURE 1. Array pneumatic separation device.

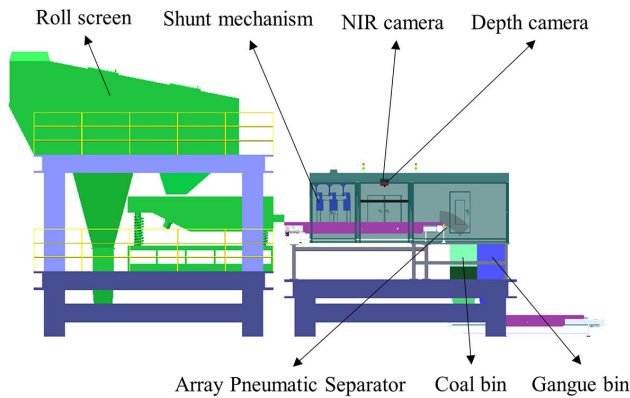


FIGURE 2. Hardware composition of the coal and gangue intelligent sorting system.

whose diameters are within the above range are screened out. We need to identify and sort this part. Second, the screened coal and gangues are transported by belt to the intelligent sorting system, and the scattered coal and gangues are approximately divided into four columns by the shunt mechanism. Third, the visual module is applied to identify coal or gangue and obtain the size information of the gangues to judge their mass and postures. The relevant parameters of gangue and the distance to be sorted are inputted into the gangue flexible sorting model to obtain the required number of air ports. Last, according to the attitude of gangues, the number of horizontal and vertical air blowing ports of the end pneumatic separation device is determined to realize the flexible sorting strategy, in which different gangues can be sorted to the appropriate position. Fig. 2 shows the hardware components of the coal and gangue intelligent sorting system:

III. ANALYSIS ON INFLUENCING FACTORS OF GANGUE MOVEMENT TRACK

Fig. 3 shows the trajectory of gangue pneumatic separation. Curve 1 shows the movement track of the gangue without the influence of high-pressure gas, and curve 2 shows the

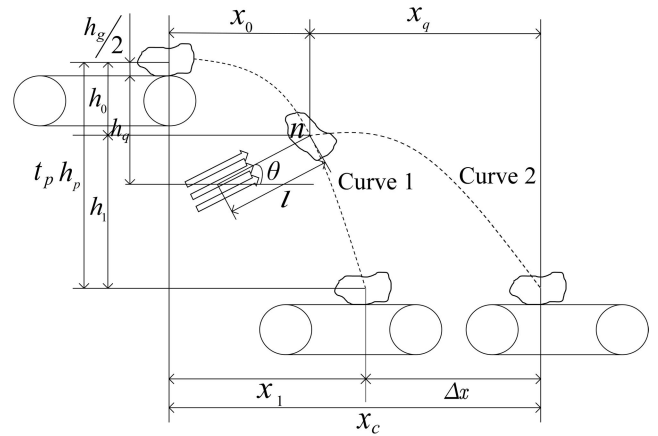


FIGURE 3. Pneumatic separation schematic diagram of gangue.

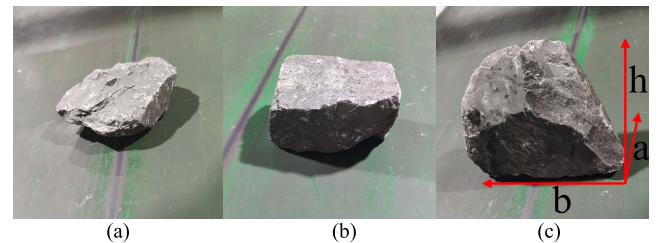


FIGURE 4. Posture classification of gangue; (a) flat posture; (b) oblate posture; (c) vertical posture.

movement track of the gangue under the action of high-pressure gas. h_g is the height of gangue, h_0 is the vertical falling height of gangue when it falls into the airflow domain, h_q is the distance between the upper part of the belt and the axis of the pneumatic separation device, h_p is the total height of gangue falling, v_0 is the speed of the belt, m is the mass of gangue, θ is the rotation angle of the pneumatic separator device, t_q is the airflow action time, x_1 is the total horizontal movement distance of gangue when it is not blown, x_c is the total horizontal movement distance of gangue after being blown, x_0 is the horizontal movement distance of gangue when it just enters the airflow domain, x_q is the horizontal movement distance of gangue after the action of airflow domain, and r is the length of the nozzle. This article takes the gangues to be sorted to a suitable position as the criterion and analyzes the factors that affect the horizontal movement distances of the gangues.

A. OBTAINING METHOD OF GANGUE POSTURE

The size and posture of gangue vary greatly, so their trajectories are also different. To ensure that the pneumatic separation method can achieve a better separation effect for all gangues, the gangues are approximately divided into three attitudes, as shown in Fig. 4, and the classification criteria are shown in Table 1.

The side of the gangue's bounding box with the same direction of belt movement is denoted as a ; the side perpendicular to the direction of belt movement is denoted as b ; the height of

TABLE 1. Classification standard of gangue posture.

| Gangue posture | Attitude classification criteria | Aspect ratio | Number of blowing ports |
|----------------|---|-------------------|-------------------------|
| Flat | $\frac{\min\{a,b\}}{h} > 1.3$ | $\frac{a}{b} = n$ | $i = \frac{n}{n+1}d$ |
| Oblate | $0.6 \leq \frac{\min\{a,b\}}{h} \leq 1.3$ | | |
| Vertical | $\frac{\min\{a,b\}}{h} < 0.6$ | $\frac{h}{b} = n$ | $j = \frac{1}{n+1}d$ |

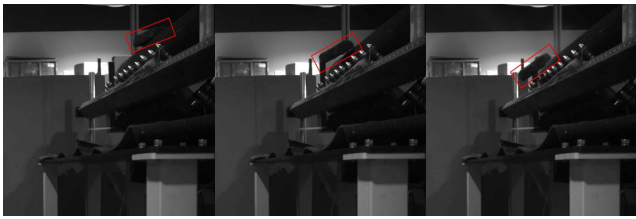


FIGURE 5. Falling posture of flat gangue.

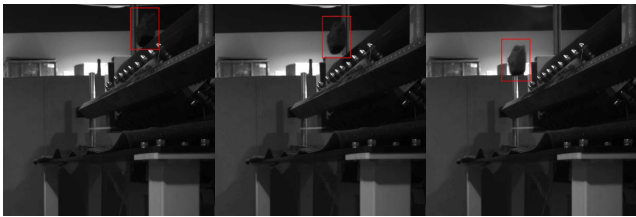


FIGURE 6. Falling posture of vertical gangue.

gangue is denoted as h ; n is the ratio of the number of vertical and horizontal blowing holes in the end sorting device; i is the number of vertical blowing holes; and j is the number of horizontal blowing holes.

The postures of the gangues on the belt are different, and the postures when it falls will also be different, as shown in Fig. 5 and Fig. 6. Different sorting strategies should be adopted for gangues with different postures.

B. ANALYSIS OF OPTIMAL BLOWING ANGLE OF PNEUMATIC SEPARATION DEVICE

In the pneumatic separation method, if the nozzle is fixed in a fixed direction at a certain position, achieving accurate sorting will be difficult due to the long horizontal movement distance of the gangue and the large gas pressure loss when the belt runs at a fast speed. For this reason, the array pneumatic separation device designed in this paper can be adjusted to different angles for sorting according to different influencing factors, reducing mis-sorting caused by gas pressure loss due to an excessively long distance.

$$y_0 = \frac{g}{2v_0^2}x_0^2 \tag{1}$$

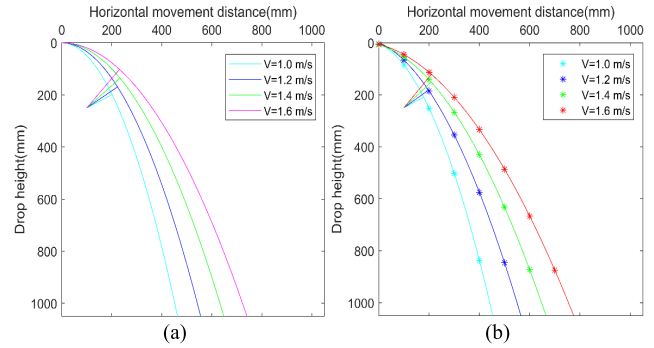


FIGURE 7. Analysis of theoretical and practical optimum blowing angle of nozzle at different belt speeds; (a) theoretical trajectory; (b) actual trajectory.

TABLE 2. Theoretical and practical optimal blowing angle of the nozzle at different belt speeds.

| Belt speed | 1.0 m/s | 1.2 m/s | 1.4 m/s | 1.6 m/s |
|-----------------------------------|---------|---------|---------|---------|
| Theoretical optimum blowing angle | 27° | 34° | 41° | 49° |
| Actual optimum blowing angle | 30° | 36° | 43° | 51° |

$$d_{\min} = (\sqrt{(x_0 - x_1)^2 + (y_0 - y_1)^2})_{\min} \tag{2}$$

$$\theta = \arctan \frac{2y_1 - gt^2}{2v_0t - 2x_1} \tag{3}$$

Equation (1) represents the theoretical trajectory curves of gangues. To minimize the energy loss of high-pressure gas in the air, the angle corresponding to the minimum distance between the axis of the pneumatic separation device and a point on the curve is the optimal blowing angle. As the time interval of different gangue falling from the belt to the nozzle is very small, this paper mainly analyzes the influence of different belt speeds on the blowing angle. This paper selects 20 pieces of gangue in each of the three postures to carry out experimental collection and theoretical simulation of their falling trajectories at different belt velocities and then obtains their average values. The theoretical and actual running trajectories are shown in Fig. 7:

According to the theory and actual running track of gangue, the optimum blowing angle corresponding to different belt speeds can be obtained from (2) and (3), as shown in Table 2:

Considering the error in the actual environment, the optimal blowing angle corresponding to the theoretical running trajectory of gangue deviates from the actual situation. Therefore, the actual experimental data are applied to make error compensation for the theoretical optimal blowing angle. The actual optimal blowing angle is obtained as shown in (4):

$$\theta = 30^\circ + (v_0 - 1) \times 35 \quad (1 \leq v_0 < 2.8) \tag{4}$$

C. ANALYSIS ON DIFFERENT INFLUENCING FACTORS OF GANGUE RUNNING TRACK BEFORE BLOWING

The horizontal movement of gangue can be divided into two stages: before blowing and after blowing. When the gangue

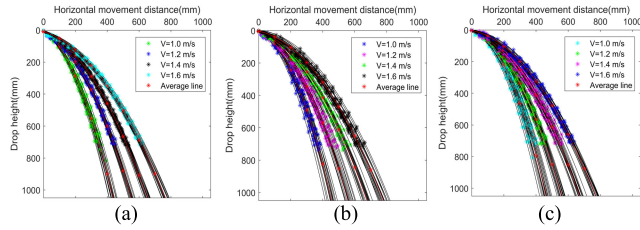


FIGURE 8. Comparison of movement trajectories of gangue with the same posture at different belt speeds; (a) falling track of flat gangue; (b) falling track of oblate gangue; (c) falling track of vertical gangue.

is thrown from the belt before blowing, it makes a horizontal projectile motion. At this time, the gangue is only affected by gravity. The falling tracks of gangue with different shapes, sizes and belt speeds are also different, and the different falling tracks correspond to different blowing angles and blowing strategies. According to the displacement formula of horizontal projectile motion, the horizontal displacement of gangue before blowing is shown in (5):

$$x_0 = v_0 \sqrt{\frac{2h_q + h_g - (r + 300v_0 - 160) \sin \theta}{1000g}} \quad (5)$$

where:

$$t_0 = \sqrt{\frac{2h_0}{g}} \quad (6)$$

$$h_0 = \frac{2h_q + h_g - 2l \sin \theta}{2000} \quad (7)$$

$$l = \frac{r}{2} + 150v_0 - 80 \quad (8)$$

1) INFLUENCE OF DIFFERENT BELT SPEEDS ON SEPARATION DISTANCE

After theoretical analysis, (5) shows that the distance of the object thrown from the belt is related to the belt velocity and height of the gangue. To ensure that gangue at different belt speeds can be sorted to the appropriate position, it is necessary to analyze the distance of gangue horizontal movement under different belt speeds. In this paper, four belt speeds are selected for the experiment, and the gangue posture and size remain constant with different belt speeds.

According to the gangues of the three previously classified postures, 20 gangues of each posture are selected as samples. The gangue with the same posture is thrown from the belt at different speeds, and a camera is utilized to collect images to obtain the central point coordinates of each position in the falling process of gangue. Fitting these points into a curve is the falling track of gangue, as shown in Fig. 8:

It can be seen from the Fig. 8 that the falling trajectories of gangue with the same posture are obviously different at different belt velocities. The faster the belt speed is, the farther the horizontal movement distance of gangue.

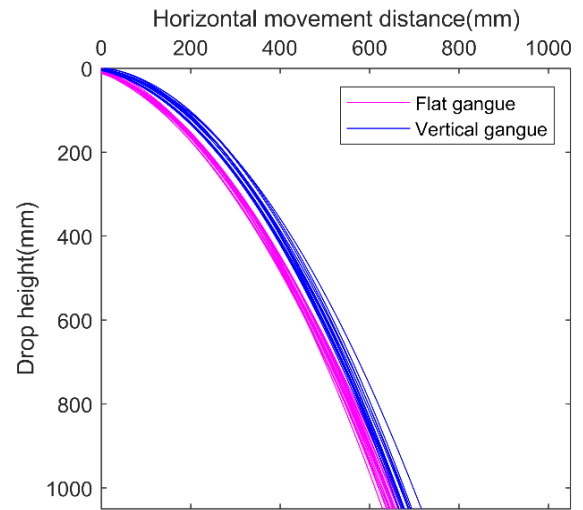


FIGURE 9. Comparison of movement trajectories of gangue with the same diameter and different postures.

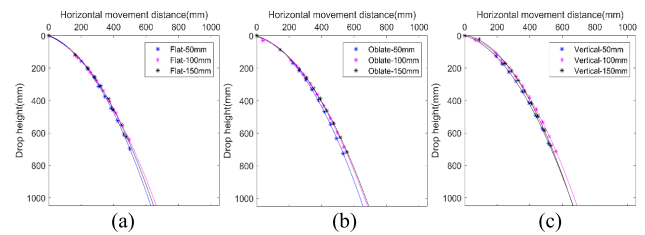


FIGURE 10. Comparison of movement trajectories of gangue with the same postures and different diameters (a) falling track of flat gangue; (b) falling track of oblate gangue; (c) falling track of vertical gangue.

2) INFLUENCE OF DIFFERENT GANGUE HEIGHTS ON SEPARATION DISTANCE

According to (5), the different heights of gangue will have a certain influence on the horizontal movement distance at the same belt speed. The higher the height of the gangue is, the farther the horizontal movement distance. In this paper, ten flat gangues and ten vertical gangues with the same diameter are selected for experimental verification. The gangues fall from the belt at the same speed, and their running tracks are shown in Fig. 9.

It can be seen from Fig. 9 that the horizontal movement distance of the vertical posture gangue is farther than that of the flat posture gangue when the diameter and belt speed are equivalent. Therefore, the difference in gangue posture has a certain influence on the horizontal movement distance of gangue, but the experimental results show that the influence is very small.

3) INFLUENCE OF DIFFERENT GANGUE DIAMETERS ON SEPARATION DISTANCE

Equation (5) shows that the horizontal movement distance of gangue before blowing is independent of the diameter of gangue. In this regard, gangue with diameters of 50 mm, 100 mm and 150 mm is selected for three postures to carry out experimental verification. The results are shown in Fig. 10:

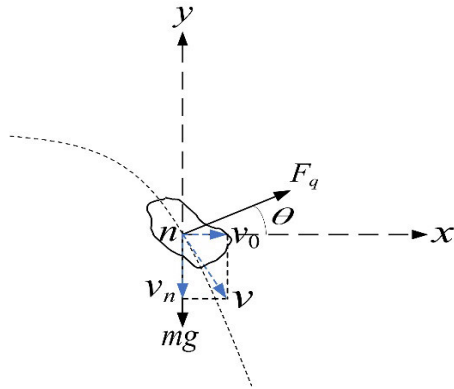


FIGURE 11. Diagram of gangue movement in airflow domain.

The experimental results show that the falling trajectories of gangue with different diameters are almost the same for the same posture and belt speed, and the diameter of gangue has no influence on the horizontal movement distance of the gangue before blowing.

From the abovementioned theoretical analysis and experimental verification, it can be seen that the belt speed is the most important factor affecting the horizontal movement distance of gangue before blowing, and the height and diameter of gangue have minimal influence on it, which can be disregarded.

D. ANALYSIS ON DIFFERENT INFLUENCING FACTORS OF GANGUE RUNNING TRACK AFTER BLOWING

To facilitate the analysis of the movement process of gangue in the airflow area, the following explanations are made: (1) Ignore the air resistance effect of the gangue in the process of falling; (2) The action time of high-pressure gas, which belongs to millisecond level, is very short. During this period, the movement distance of gangue is not considered; (3) During the action time of high-pressure gas, the gas pressure is regarded as a constant force.

1) KINEMATIC ANALYSIS OF GANGUE IN AIRFLOW FIELD

When the gangue falls into the airflow area, it is affected not only by gravity but also by airflow pressure. The force acting on gangue in the airflow area is approximately shown in Fig. 11:

The force of high-pressure gas acting on gangue is denoted as F_q . When the gangue enters the airflow domain, the speed in the y direction is recorded as v_n , F_q and v_n can be expressed by (9) and (10) respectively:

$$F_q = p \sum_{j=1}^d M_j \quad (9)$$

$$v_n = \sqrt{2gh_0} \quad (10)$$

According to Newton's second law, the horizontal and vertical accelerations of gangue in the airflow domain are

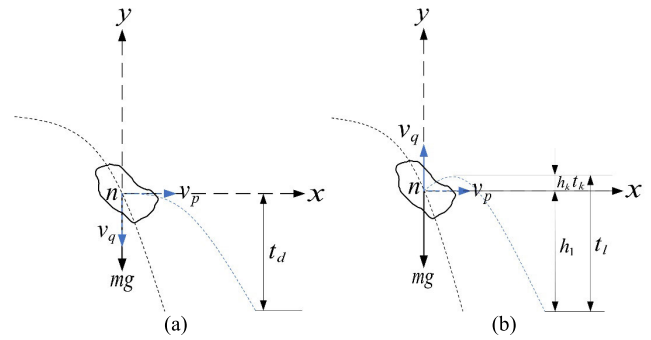


FIGURE 12. Diagram of gangue movement after leaving the airflow domain; (a) $v_q < 0$; (b) $v_q > 0$.

shown in (11):

$$\begin{aligned} a_x &= \frac{F_q \cos \theta}{m} \\ a_y &= \frac{F_q \sin \theta - mg}{m} \end{aligned} \quad (11)$$

After the high-pressure gas acting force ends, the motion trajectory of gangue will change. At this time, the horizontal and vertical motion velocity of gangue can be obtained from (12) and (13) respectively:

$$v_p = v_0 + \int_0^{t_q} a_x dt = v_0 + \frac{F_q t_q \cos \theta}{m} \quad (12)$$

$$v_q = -v_n + \int_0^{t_q} a_y dt = -\sqrt{2gh_0} + \frac{(F_q \sin \theta - mg)t_q}{m} \quad (13)$$

2) KINEMATIC ANALYSIS OF GANGUE AFTER LEAVING THE AIRFLOW DOMAIN

After the high-pressure gas acting force ends, the gangue continues to make horizontal throwing movements. At this time, the movement of the gangue can be divided into two situations: the vertical velocity $v_q < 0$ and $v_q > 0$. When $v_q < 0$, the movement trajectory of gangue is shown in Fig. 12 (a), and the gangue accelerates to drop to the lower belt. At this time, the height of the gangue from the belt below and the time of gangue falling on the belt can be obtained by (14) and (15), and the horizontal movement distance of the gangue can be expressed by (16).

$$h_1 = -v_q t_d + \frac{1}{2} g t_d^2 \quad (14)$$

$$t_d = \frac{v_q + \sqrt{v_q^2 + 2gh_1}}{g} \quad (15)$$

$$x_q = \left(v_0 + \frac{F_q t_q \cos \theta}{m} \right) \frac{v_q + \sqrt{v_q^2 + 2g(h_p - h_0)}}{g} \quad (16)$$

When $v_q > 0$, the movement trajectory of gangue is shown in Fig. 12 (b). First, the gangue rises to the highest point and then freefalls to the belt below. The rising height of gangue is denoted as h_k , and the required time is t_k . The falling height of gangue from the highest point to the lower belt is $h_k + h_1$,

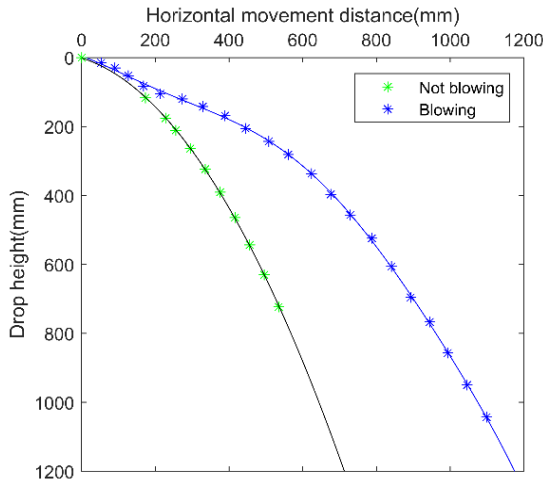


FIGURE 13. Comparison of falling track of gangue after pneumatic separation and free sliding.

and the required time is t_l , which can be obtained from (17) to (19). The horizontal movement distance x_q of gangue can be expressed by (19):

$$h_k + h_1 = \frac{1}{2}gt_l^2 \tag{17}$$

$$t_k = \frac{a_y t_q - v_n}{g} \tag{18}$$

$$t_l = \frac{\sqrt{v_q^2 + 2g(h_p - h_0)}}{g} \tag{19}$$

(20), as shown at the bottom of the next page, where:

$$h_0 = \frac{2h_q + h_g - (r + 300v_0 - 160) \sin \theta}{2000} \tag{21}$$

$$v_q = -\sqrt{2gh_0} + \frac{(F_q \sin \theta - mg)t_q}{m} \tag{22}$$

$$m = \rho v \tag{23}$$

It can be seen from the above formula that the horizontal movement distance of the gangue being blown is related to a series of variables, including belt speed, gangue height, gangue mass, blowing force, blowing time, and the distance between the axis of the pneumatic separation device and the upper part of the belt. In this paper, the distance between the axis of pneumatic separation device and the top of the belt are set as fixed values. Therefore, if the gangue needs to be sorted to an appropriate position when the belt speed, gangue height and gangue quality are different, there should be corresponding different forces and different blowing times to realize flexible sorting for different sizes of gangue. Fig. 13 shows a comparison of the actual falling track of gangue after pneumatic separation and free falling:

IV. CONSTRUCTION AND OPTIMIZATION OF FLEXIBLE SEPARATION MATHEMATICAL MODEL FOR GANGUE

A. MODEL ESTABLISHMENT

According to the horizontal movement distances x_0 and x_q of gangue before and after blowing, the total horizontal

movement distance x_c of gangue falling from the belt can be obtained, which is expressed by (24) and (25):

When $v_q < 0$,

$$x_c = v_0 \sqrt{\frac{2h_q + h_g - (r + 300v_0 - 160) \sin \theta}{1000g}} + \left(v_0 + \frac{F_q t_q \cos \theta}{m} \right) \frac{v_q + \sqrt{v_q^2 + 2g(h_p - h_0)}}{g} \tag{24}$$

When $v_q > 0$, (25), as shown at the bottom of the next page.

For gangues of different postures and sizes under different influencing factors, to sort them to an appropriate position, this paper sets the horizontal movement distance x_c of gangue as a variable, sets the distance that gangue needs to be sorted, and then the sorting force is obtained according to different characteristic parameters of different gangues. In this regard, Equations (24) and (25) are transformed into (26), which considers the belt speed, gangue height, gangue mass, distance of gangue being sorted and blowing time as variables, and the required blowing force F_q as the output result. After the required blowing force is obtained, the total number of blowing ports d can be obtained according to (27). The blowing quantity of transverse and longitudinal blowing ports of the end pneumatic separation device is determined according to Table 1. In this way, gangue of different sizes, postures and different influencing factors can be sorted to suitable positions.

$$F_q = f(v_0, h_g, m, x_c, t_q) \tag{26}$$

$$d = \frac{f(v_0, h_g, m, x_c, t_q)}{PM_q} \tag{27}$$

In this equation, M_q is the cross-sectional area of the nozzle, and P is the gas pressure. The advantage of this model is that gangues with randomly distributed sizes and postures can be sorted to an appropriate position under various influencing factors and that flexible sorting for all kinds of gangue can be realized.

B. MODEL OPTIMIZATION

Due to the uncertainty of theoretical assumptions, there is a certain error between the calculation results of the theoretical model and the actual scene. To reduce the error, parameters k_1 , k_2 and constant b_1 are introduced in this paper. k_1 and k_2 respectively correspond to the coefficients of horizontal movement distance of gangue before blowing and after blowing. The three parameters are adjusted by experiments so that the theoretical value and experimental value are suitable. The horizontal movement formula of gangue with correction coefficient is shown in (28):

$$x_r = k_1 x_0 + k_2 x_q + b_1 \tag{28}$$

This paper selects gangue with different postures and sizes to carry out experiments at different belt velocities

and obtains the actual running distance of gangue before and after blowing. Then the theoretical running distance of gangue before and after blowing is calculated by the theoretical formula and compared with the actual running distance, as shown in Table 3. In the table, N represents the experimental sequence number; v represents the belt velocity, p represents the gangue posture; s represents the diameter of gangue; A and B respectively represent the theoretical horizontal movement distance of gangue before blowing and after blowing; C and D respectively represent the actual horizontal movement distance of gangue before and after blowing. e represents the theoretical sorting distance of gangue, and f represents the actual sorting distance of gangue.

The experimental results show that there is a certain error between the theoretical sorting distance and the actual sorting distance under different belt speeds, different gangue postures and different gangue sizes. The error can be divided into two parts: before blowing and after blowing. According to the experimental results, the values of parameters k_1 , k_2 and constant b_1 are adjusted to reduce the errors, so as to improve the accuracy and robustness of the model. Substituting the data in the table into (29) - (31), the values of k_1 , k_2 and b_1 can be obtained as 0.85, 0.764 and 0.00487 respectively.

$$k_1 = \frac{1}{N} \sum_{i=1}^N \frac{C_i}{A_i} \tag{29}$$

$$k_2 = \frac{1}{N} \sum_{i=1}^N \frac{D_i}{B_i} \tag{30}$$

$$b_1 = \frac{1}{N} \sum_{i=1}^N (f_i - k_1 A_i - k_2 B_i) \tag{31}$$

The modified horizontal movement distance formula of gangue is shown in (32):

$$x_r = 0.85x_0 + 0.764x_q + 0.00487 \tag{32}$$

The horizontal movement distance of gangue after error compensation is substituted into (27) to obtain the gangue sorting model in the actual application scenario, as shown in (33). Model modification has important guiding significance and practical value for the pneumatic separation of

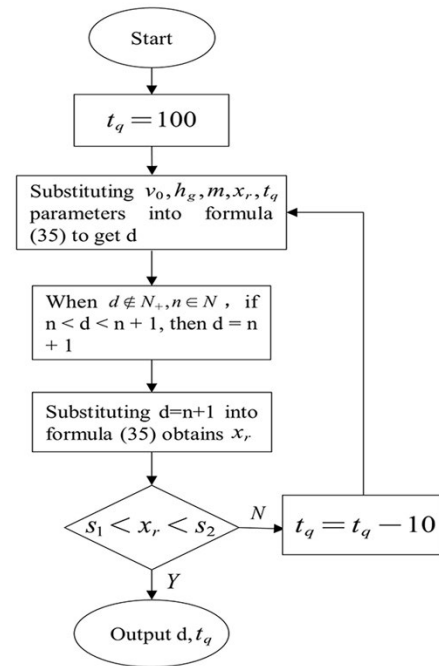


FIGURE 14. Coordinated control strategy for the number of puff ports and the blowing time of the pneumatic separation device.

gangue.

$$d = \frac{f(v_0, h_g, m, x_r, t_q)}{PM_q} \tag{33}$$

According to (33), the number of puff ports of the pneumatic separation device is d , but the calculated d may not be an integer value. Therefore, this paper proposes the coordinated control strategy of the number of puff ports and the blowing time as shown in Fig. 14. In this way, the optimal blowing time and the number of puff ports needed for different gangue to be sorted to an appropriate position are output.

V. EXPERIMENTAL COMPARISON AND RESULT ANALYSIS

A. FEASIBILITY ANALYSIS OF PNEUMATIC SEPARATION SCHEME IN HIGH SPEED SCENARIO

Due to the fast movement of the belt on the gangue separation line and the different shapes and sizes of gangue,

$$x_q = \left(v_0 + \frac{F_q t_q \cos \theta}{m} \right) \left(\frac{F_q t_q \sin \theta - mgt_q - m\sqrt{2gh_0} + m\sqrt{v_q^2 + 2g(h_p - h_0)}}{mg} \right) \tag{20}$$

$$x_c = v_0 \sqrt{\frac{2h_q + h_g - (r + 300v_0 - 160) \sin \theta}{1000g}} + \left(v_0 + \frac{F_q t_q \cos \theta}{m} \right) \left(\frac{F_q t_q \sin \theta - mgt_q - m\sqrt{2gh_0} + m\sqrt{v_q^2 + 2g(h_p - h_0)}}{mg} \right) \tag{25}$$

TABLE 3. Comparison of theoretical and practical sorting distances of gangue with different speeds, postures and sizes.

| (a) | | | | | | | | | |
|-----|---------|----------|-------|--------|--------|-------|-------|---------|-------|
| N | v (m/s) | p | s(mm) | A(mm) | B(mm) | C(mm) | D(mm) | e(mm) | f(mm) |
| 1 | 1.0 | Flat | 50 | 211.89 | 814.82 | 168 | 636 | 1026.75 | 804 |
| 2 | | | 100 | 209.47 | 680.50 | 172 | 553 | 889.97 | 725 |
| 3 | | Oblate | 50 | 214.30 | 749.53 | 189 | 481 | 963.83 | 670 |
| 4 | | | 100 | 215.80 | 581.16 | 181 | 455 | 797.03 | 636 |
| 5 | | Vertical | 50 | 222.50 | 745.93 | 203 | 487 | 968.40 | 690 |
| 6 | | | 100 | 225.88 | 632.54 | 205 | 435 | 858.40 | 640 |
| (b) | | | | | | | | | |
| N | v (m/s) | p | s(mm) | A(mm) | B(mm) | C(mm) | D(mm) | e(mm) | f(mm) |
| 7 | 1.2 | Flat | 50 | 237.39 | 922.37 | 191 | 772 | 1159.76 | 963 |
| 8 | | | 100 | 234.30 | 793.76 | 199 | 613 | 1028.06 | 812 |
| 9 | | Oblate | 50 | 240.46 | 848.33 | 209 | 595 | 1088.79 | 804 |
| 10 | | | 100 | 242.52 | 650.62 | 202 | 524 | 893.14 | 726 |
| 11 | | Vertical | 50 | 250.95 | 843.91 | 216 | 544 | 1094.90 | 760 |
| 12 | | | 100 | 255.28 | 716.4 | 219 | 447 | 971.67 | 666 |
| (c) | | | | | | | | | |
| N | v (m/s) | p | s(mm) | A(mm) | B(mm) | C(mm) | D(mm) | e(mm) | f(mm) |
| 13 | 1.4 | Flat | 50 | 252.07 | 1040.5 | 218 | 873 | 1292.59 | 1091 |
| 14 | | | 100 | 248.07 | 897.44 | 210 | 758 | 1145.52 | 968 |
| 15 | | Oblate | 50 | 256.01 | 957.39 | 228 | 685 | 1213.46 | 913 |
| 16 | | | 100 | 259.20 | 737.95 | 224 | 577 | 997.15 | 801 |
| 17 | | Vertical | 50 | 269.33 | 951.61 | 230 | 633 | 1220.94 | 863 |
| 18 | | | 100 | 274.85 | 809.40 | 237 | 579 | 1084.22 | 816 |
| (d) | | | | | | | | | |
| N | v (m/s) | p | s(mm) | A(mm) | B(mm) | C(mm) | D(mm) | e(mm) | f(mm) |
| 19 | 1.6 | Flat | 50 | 252.80 | 1168.7 | 209 | 1035 | 1421.48 | 1244 |
| 20 | | | 100 | 247.60 | 1012.6 | 197 | 918 | 1260.20 | 1115 |
| 21 | | Oblate | 50 | 257.93 | 1076.4 | 221 | 827 | 1334.48 | 1048 |
| 22 | | | 100 | 260.40 | 838.23 | 220 | 753 | 1098.64 | 973 |
| 23 | | Vertical | 50 | 277.45 | 1062.7 | 234 | 806 | 1339.90 | 1040 |
| 24 | | | 100 | 282.12 | 911.4 | 237 | 745 | 1193.50 | 982 |

it is difficult to realize the flexible sorting of gangue on the high-speed belt with the current robot technology. The pneumatic separation method proposed in this paper utilizes the characteristics of a high-frequency solenoid valve, such as high response speed, low control difficulty, and stable and reliable work, combined with the flexible sorting model established in this paper and the array pneumatic separation device, which can realize the flexible sorting of gangue on a high-speed belt. Table 4 shows a comparison of the sorting parameters between the series-parallel robot and the array pneumatic separation device proposed in this paper:

It can be seen from the data in the table that the sorting speed and sorting efficiency of the series-parallel robot are difficult to realize the function of fast grasping on

the high-speed belt and that its control complexity is relatively high. However, the array pneumatic separation device employed in this paper has the advantages of high frequency, large sorting quantity and low sorting complexity, which meets the demand for high-speed sorting of gangue.

B. VALIDITY VERIFICATION OF GANGUE FLEXIBLE SORTING STRATEGY BASED ON MULTI-INFORMATION FUSION

To verify the performance and sorting accuracy of the flexible sorting method proposed in this paper, 450 pieces of gangue were selected for the pneumatic separation experiment on a high-speed belt. The experiment was divided into three groups, and the experimental results are shown in Table 5.

TABLE 4. Performance comparison between array pneumatic separation device and series-parallel robot.

| Belt speed | Sorting device | | Frequency (times/min) | Sorting quantity (min) | Sorting complexity |
|------------|---------------------------|----------------|--------------------------|------------------------|--------------------|
| 1.2 m/s | Robot | Serial robot | 22 | 15 | Difficult |
| | | Parallel robot | 200 | 120 | Difficult |
| | Array pneumatic separator | | 4800 | 1080 | Easy |
| 1.4 m/s | Robot | Serial robot | 22 | 15 | Difficult |
| | | Parallel robot | 200 | 120 | Difficult |
| | Array pneumatic separator | | 4800 | 1260 | Easy |
| 1.6 m/s | Robot | Serial robot | 22 | 15 | Difficult |
| | | Parallel robot | 200 | 120 | Difficult |
| | Array pneumatic separator | | 4800 | 1440 | Easy |

TABLE 5. Experimental verification of gangue flexible sorting strategy based on multi-information fusion.

| Device | Belt speed (m/s) | Number of samples | Sorting performance | Sorting accuracy |
|--|---------------------|----------------------|------------------------|---------------------|
| NIR camera + Pneumatic separator | 1.4 | 450 | 0.8467 | 0.8058 |
| NIR camera + Depth camera + Pneumatic separator | | | 0.9356 | 0.8646 |
| NIR camera + Depth camera + Flexible sorting model | | | 0.9578 | 0.9466 |
| + Pneumatic separator | | | | |

Among them, sorting performance refers to the ratio of the number of gangues that can be acted on by gas pressure to the total number of gangues, which is to verify the reliability of the high-speed coal and gangue sorting system. Sorting accuracy refers to the proportion of gangue that can be sorted to the proper position among the gangue that can be affected by high-pressure gas. This proportion mainly verifies the reliability of the flexible sorting model based on the sorting performance.

As seen from Table 5, the combination of a near-infrared camera and the pneumatic separation method can realize the rapid sorting of gangue under a high-speed belt, but the sorting accuracy is low. However, with the addition of depth camera, flexible sorting model and array pneumatic separation device, the sorting performance and sorting accuracy of the system are greatly improved. In this way, the function of quick and accurate sorting of gangue with different shapes and sizes can be realized for the operation of a high-speed belt.

VI. CONCLUSION

The separation of coal and gangue is an indispensable link in the process of coal production. To solve the problem that it is difficult for current methods to realize the rapid and accurate sorting of a large amount of gangue with random shapes and sizes on a high-speed belt, an online flexible sorting model for coal and gangue based on the fusion of near-infrared and depth image information is proposed in this paper. This paper adopts the combination of near-infrared

camera and depth camera to realize the identification of coal and gangue and the acquisition of gangue posture information respectively. According to the information obtained by the cameras, the method of pneumatic separation is adopted to realize the sorting of coal and gangue on a high-speed belt. However, the current pneumatic separation of coal and gangue only adopts a single sorting scheme, and the sizes and postures of gangue vary greatly, so it is difficult to realize that each gangue can be sorted to an appropriate position by only one sorting strategy. In this regard, a mathematical model of gangue flexible sorting is established, and an array pneumatic separation device is designed.

First, this paper conducts a theoretical analysis of the movement trajectories of gangue with different sizes and postures for different influencing factors and determines the factors affecting the horizontal movement distance of gangue through experimental verification. Second, the theoretical mathematical formula of the horizontal movement distance of gangue pneumatic separation is established, and a flexible separation model is obtained. The relevant information of gangue obtained by the camera and the different factors affecting the horizontal movement distance of gangue are taken as the input variables of the model, and the output is the different flexible sorting strategy for each gangue to realize the rapid and accurate sorting of gangue with different shapes and sizes on a high-speed belt. The actual experimental data are employed to compensate the error of the theoretical flexible sorting model of gangue to make it suitable for sorting work in actual scenes. In addition, this paper proposes a

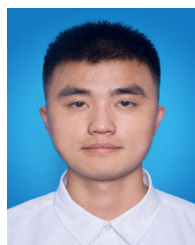
coordinated control strategy between the number of blowing ports and the blowing time of pneumatic separation device to realize closed-loop control of the flexible sorting strategy of gangue. Last, through experimental verification, the flexible sorting model can effectively improve the sorting accuracy of gangue. Overall, the flexible sorting model of gangue based on multi-information fusion proposed in this paper can realize accurate sorting of gangue with different shapes and sizes in high-speed dynamic scenes.

ACKNOWLEDGMENT

(Zixiang Wang and Shuxin Xie contributed equally to this work.)

REFERENCES

- [1] G. Fan, D. Zhang, and X. Wang, "Reduction and utilization of coal mine waste rock in China: A case study in Tiefsa coalfield," *Resour. Conservation Recycling*, vol. 83, pp. 24–33, Feb. 2014.
- [2] Y. Yang, Q. Zeng, G. Yin, and L. Wan, "Vibration test of single coal gangue particle directly impacting the metal plate and the study of coal gangue recognition based on vibration signal and stacking integration," *IEEE Access*, vol. 7, pp. 106784–106805, 2019.
- [3] E. J. Meyer and I. K. Craig, "Dynamic model for a dense medium drum separator in coal beneficiation," *Minerals Eng.*, vol. 77, pp. 78–85, Jun. 2015.
- [4] W. M. Ambrós, "Jigging: A review of fundamentals and future directions," *Minerals*, vol. 10, no. 11, p. 998, Nov. 2020.
- [5] Y. Zhou, B. Albijanic, B. Tadesse, Y. Wang, J. Yang, and X. Zhu, "Surface properties of aged coal and their effects on bubble–particle attachment during flotation," *Adv. Powder Technol.*, vol. 31, no. 4, pp. 1490–1499, Apr. 2020.
- [6] Y. Zhao, X. Yang, Z. Luo, C. Duan, and S. Song, "Progress in developments of dry coal beneficiation," *Int. J. Coal Sci. Technol.*, vol. 1, no. 1, pp. 103–112, Mar. 2014.
- [7] L. Zou, X. Yu, M. Li, M. Lei, and H. Yu, "Nondestructive identification of coal and gangue via near-infrared spectroscopy based on improved broad learning," *IEEE Trans. Instrum. Meas.*, vol. 69, no. 10, pp. 8043–8052, Apr. 2020.
- [8] H. Yang and Z. Qiao, "Design of separation system of coal and gangue based on X-ray and machine vision," *Ind. Mine Autom.*, vol. 43, no. 3, pp. 85–89, 2017.
- [9] Y. Yang and Q. Zeng, "Multipoint acceleration information acquisition of the impact experiments between coal gangue and the metal plate and coal gangue recognition based on SVM and serial splicing data," *Arabian J. Sci. Eng.*, vol. 46, no. 3, pp. 2749–2768, Mar. 2021.
- [10] Z. Ding, G. Chen, Z. Wang, W. Chi, Z. Wang, and Y. Fan, "A real-time multilevel fusion recognition system for coal and gangue based on near-infrared sensing," *IEEE Access*, vol. 8, pp. 178722–178732, 2020.
- [11] Y. Pu, D. B. Apel, A. Szmigiel, and J. Chen, "Image recognition of coal and coal gangue using a convolutional neural network and transfer learning," *Energies*, vol. 12, no. 9, p. 1735, May 2019.
- [12] W. Li, Y. Wang, B. Fu, and Y. Lin, "Coal and coal gangue separation based on computer vision," in *Proc. 5th Int. Conf. Frontier Comput. Sci. Technol.*, Aug. 2010, pp. 467–472.
- [13] C. Aldrich, G. T. Jemwa, J. C. van Dyk, M. J. Keyser, and J. H. P. van Heerden, "Online analysis of coal on a conveyor belt by use of machine vision and kernel methods," *Int. J. Coal Preparation Utilization*, vol. 30, no. 6, pp. 331–348, Nov. 2010.
- [14] S. Lei, X. Xiao, M. Zhang, and J. Dai, "Visual classification method based on CNN for coal-gangue sorting robots," in *Proc. 5th Int. Conf. Autom., Control Robot. Eng. (CACRE)*, Sep. 2020, pp. 543–547.
- [15] D. Dou, D. Zhou, J. Yang, and Y. Zhang, "Coal and gangue recognition under four operating conditions by using image analysis and relief-SVM," *Int. J. Coal Preparation Utilization*, vol. 40, no. 7, pp. 473–482, Jul. 2020.
- [16] G. Wang, T. Su, W. Liu, Z. Qian, and J. Li, "Design of intelligent coal and gangue sorting system based on EAIKD," *Ind. Mine Autom.*, vol. 46, no. 1, pp. 105–108, 2020.
- [17] X. Cao, J. Fei, and P. J. C. S. T. Wang, "Study on coal-gangue sorting method based on multi-manipulator collaboration," *Coal Sci. Technol.*, vol. 47, no. 4, pp. 7–12, 2019.
- [18] D. Shang, Y. Wang, Z. Yang, J. Wang, and Y. Liu, "Study on comprehensive calibration and image sieving for coal-gangue separation parallel robot," *Appl. Sci.*, vol. 10, no. 20, p. 7059, Oct. 2020.
- [19] J. Peng, X. Tang, B. Chen, F. Jiang, Y. Yang, R. Zhang, D. Gao, X. Zhang, and Z. Huang, "Failure type prediction using physical indices and data features for solenoid valve," *Appl. Sci.*, vol. 10, no. 4, p. 1323, Feb. 2020.
- [20] J. X. Zhang, T. Chen, Z. D. Yu, and W. Li, "Xinjiang cotton seed color separation system based on computer vision," *Trans. Chin. Soc. Agricult. Machinery*, vol. 40, no. 10, pp. 161–164, 2009.
- [21] M. Baigvand, A. Banakar, S. Minaei, J. Khodaei, and N. Behroozi-Khazaei, "Machine vision system for grading of dried figs," *Comput. Electron. Agricult.*, vol. 119, pp. 158–165, Nov. 2015.
- [22] H. Bi, H. Zhu, L. Zu, S. He, Y. Gao, and S. Gao, "Pneumatic separation and recycling of anode and cathode materials from spent lithium iron phosphate batteries," *Waste Manage. Res., J. Sustain. Circular Economy*, vol. 37, no. 4, pp. 374–385, Apr. 2019.
- [23] N. Hayashi and T. Oki, "Effect of orifice introduction on the pneumatic separation of spherical particles," *Mater. Trans.*, vol. 55, no. 4, pp. 700–707, 2014.
- [24] E. de Almeida, N. Spogis, O. P. Taranto, and M. A. Silva, "Theoretical study of pneumatic separation of sugarcane bagasse particles," *Biomass Bioenergy*, vol. 127, Aug. 2019, Art. no. 105256.
- [25] K. Zheng, C. Du, J. Li, B. Qiu, and D. Yang, "Underground pneumatic separation of coal and gangue with large size (≥ 50 mm) in green mining based on the machine vision system," *Powder Technol.*, vol. 278, pp. 223–233, Jul. 2015.
- [26] K. Zheng, C. Du, J. Li, and B. Qiu, "Coal and gangue underground pneumatic separation effect evaluation influenced by different airflow directions," *Adv. Mater. Sci. Eng.*, vol. 2016, pp. 1–13, Jan. 2016.



ZIXIANG WANG was born in 1997. He received the B.E. degree from Yangzhou University, China, in 2019. He is currently pursuing the M.E. degree with the School of Mechanical and Electrical Engineering, Soochow University. His research interests include robot vision and robotics.



SHUXIN XIE was born in 1980. He received the B.E. degree from the School of Material Engineering, in 2003, and the M.S. degree from the School of Mechanical and Electrical Engineering, Soochow University, Suzhou, China, in 2010, where he is currently pursuing the Ph.D. degree in intelligent robot technology. His research interests include robot vision and motion planning.



GUODONG CHEN was born in 1983. He received the Ph.D. degree from the Harbin Institute of Technology, Harbin, China, in 2011. He is currently an Associate Professor with Soochow University. His research interests include robot vision and intelligent industrial robots.



ZIHAO DING was born in 1996. He received the B.Sc. degree from Wuhan Textile University, China, in 2017. He is currently pursuing the Ph.D. degree with the School of Mechanical and Electrical Engineering, Soochow University. His research interests include robot vision and robotics.



WENZHENG CHI (Member, IEEE) received the B.E. degree in automation from Shandong University, Jinan, China, in 2013, and the Ph.D. degree in biomedical engineering from the Department of Electronics Engineering, The Chinese University of Hong Kong, Hong Kong, in 2017. Her research interests include mobile robot path planning, intelligent perception, and human-robot.



PENG WANG was born in 1997. He received the B.E. degree from the Wenzhen College, Soochow University, China, in 2018. He is currently pursuing the M.E. degree with the School of Mechanical and Electrical Engineering, Soochow University. His research interests include machine vision and robotics.

...